CORROSION SCIENCE AND TECHNOLOGY, Vol.2, No.1(2003), pp.18~25

Effects of Sigma (σ) Phase on the Pitting Corrosion of 25% Cr Duplex Stainless Steel; Investigations by means of Electrochemical Noise Measurement

Chan-Jin Park, Hyuk-Sang Kwon, and Hee-San Kim*

Dept. of Materials Science and Engineering, Korea Advanced Institute of Science and Technology
373-1, Kusong-dong, Yusong-gu, Taejon 305-701, Korea
**POSCO Terchnical Research Lab.*
Koedong-dong, Nam-gu, Pohang 790-785, Korea

Effects of the precipitation of σ phase on the metastable pitting as a precursor of stable pitting corrosion and also on the progress of stale pitting of the 25Cr-7Ni-3Mo-0.25N duplex stainless steel were investigated in chloride solution. Electrochemical potential and current noises of the alloy were measured in 10 % ferric chloride solution ($FeCl_3$) with zero resistance ammeter (ZRA), and then analyzed by power spectral density (PSD) and by corrosion admittance (A_c) spectrum. With aging at 850 ℃, the passive film of the alloy was found to get significantly unstable as represented by power spectral density (PSD) and a transition from metastable pitting state to stable one was observed. In the corrosion admittance spectrum, the number of negative A_c corresponding to the state of localized corrosion increased with aging, suggesting that the precipitation of σ phase considerably degraded the passive film by depleting Cr and Mo around it at α/σ or γ/σ phase boundaries, thereby leading to the initiation of the pitting corrosion. However, the Cr and Mo at α/σ or γ/σ phase boundaries which were once depleted due to the precipitation of the σ phase were partly replenished by the diffusion of Cr and Mo from the surrounding matrix with aging time longer. The initiation of pitting seems to be associated with the precipitation density of the σ phase with an effective size needed to induce the sufficient depletion of Cr and Mo around it.

Keywords : *duplex stainless steel; sigma (σ) phase; metastable pitting; electrochemical noise; power spectral density; corrosion admittance*

1. Introduction

Austenitic-ferritic duplex stainless steel (DSS) is very attractive as a structural material in the fields of energy/ environmental systems where both high mechanical strength and excellent resistance to localized and stress corrosion are required. Generally, these alloys have two to three times higher yield strength and exhibit greater resistance to localized and stress corrosion than type 300-series austenitic stainless steels at a comparable cost.

Commercial DSS usually contain 22-25 % Cr, 5-7 % Ni, 3-4 % Mo and 0.15-0.35 % N, and recent trends for newly developed DSS are towards increasing the Cr and Mo content of the alloys to improve the resistance to localized and stress corrosion. However, the increase of Cr and Mo content in DSS promote the precipitation of second phases such as sigma (σ), chi (χ) and alpha prime (α′) phases when exposed temperatures of 300 ~ 900 ℃.[1)-3)] Above all, the σ phase, a body-centered, tetragonal intermetallic compound that is rich in Cr and Mo with a larger volume fraction than any other phases is considered as the most detrimental one in the alloys.

It is well known that mechanical properties of DSS can be deteriorated seriously by the formation of small amounts of σ phase.[3),6)] Thus, the production of thick pipes or bars with large diameters is limited because of the precipitation of the σ phase in the interior of products where the cooling rate is relatively slow after solution annealing. The precipitation of σ phase also depletes surrounding phases of Cr and Mo, leading to a reduction in corrosion resistance of DSS.[6)-9)]

In conventional stainless steels, non-metallic inclusion, typically manganese sulphide (MnS) has been considered as a preferential site for pitting corrosion. Szklarska-Smialowska et al.[10)] suggested the near-surface sulphide inclusion covered with defective film in comparison with that covering the adjacent stainless steel matrix. A salt (chloride) layer is formed over the defective area, which

is accomplished by the transport of metallic ions through the defective film and their reaction with the chloride. The hydrolysis of the chloride leads to acidification. The acid formed dissolves the defective film, and begins to attack the manganese sulphide inclusion and the stainless steel surrounding the inclusion. The pit will propagate when the acidity has reached a level at which repassivation of stainless steel surface cannot occur.

However, with development of refining process for modern super stainless steels with impurity level controlled below 50 ppm, the risk of pitting corrosion at such site as MnS inclusion has been remarkably reduced. For DSS, instead, second phases such as sigma (σ) phase precipitated during improper heat treatment or welding become much influential on the pitting corrosion of the alloy. This is due predominantly to depletion of chromium (Cr) or molybdenum (Mo) around such phases.[6),9)]

Kwon et al.[11)] reported that the resistance to pitting and stress corrosion of 25 % Cr DSS was degraded remarkably with aging at 850 ℃. They suggested that the deterioration in resistance to localized corrosion of the alloy is due to the precipitation of σ phase at austenite (γ) / ferrite (α) or ferrite (α) / ferrite (α) boundaries, and additionally the precipitation kinetics of such phase can be delayed by partial substitution of tungsten (W) for molybdenum (Mo) in DSS. In spite of large amount of previous studies on the effects of σ phase on the corrosion resistance of DSS, few attempts were made to study how pit initiate and propagate at the vicinity of σ phase systematically. Nevertheless, to gain information of the initial stage of pitting, especially metastable pitting near such phase is very important to understand the effect of second phase on the localized or stress corrosion of DSS.

Recently, electrochemical noise measurement (ENM) technique has been widely used for a study on the pit stability of conventional austenitic stainless steels.[12)-15)] Specifically, the potential or current transients in time domain is closely associated with the initiation and following repassivation of metastable pit. However, so far, for DSS, a study on the pitting by means of the electrochemical noise measurement has been rarely conducted.

The objective of the present study is to investigate the effects of σ phase on the metastable pitting as a precursor of stable pitting corrosion and additionally on the further progress of stable pitting of 25Cr-7Ni-3Mo-0.25N alloy in chloride solution by means of electrochemical noise measurement.

2. Experimental

The alloy used in this study was high-purity heats melted in a laboratory-scale vacuum induction furnace, and cast in 25 kg ingots. Chemical compositions of the alloy are presented in Table 1. The alloy was prepared in the form of hot-rolled sheet 4 mm thick. The alloy was solution annealed for 2 h at 1050 ℃, and then aged respectively for 20 min, 1 h and 10 h at 850 ℃.

Table 1. Chemical compositions of experimental alloy in weight-%

Cr	Ni	Mo	N	Fe
24.60	6.60	3.12	0.25	bal.

Electrochemical potential and current vs. time of the alloy were measured in 10 % $FeCl_3 \cdot 6H_2O$ solution at 60 ℃ with a sampling time of 1 s for all data acquisition, and then analyzed quantitatively by maximum entropy method (MEM)[16)] and by corrosion admittance (Ac) spectrum.[17)]

The test specimen of interest with an exposure area of 0.5 cm^2; a working electrode, was coupled with a thin platinum (Pt) wire with a tip diameter of about 100 μm, and both electrodes were connected via zero resistance ammeter (ZRA). Very thin Pt wire was used as a cathode to reduce the contaminating noise from the cathode and to minimize the shift of corrosion potential of the working electrode affected by the inert noble electrode.[17)]

In order to measure the degree of sensitization around the σ precipitates of the DSS with aging at 850 ℃, a double-loop electrochemical potentiodynamic reactivation (DL-EPR) test was conducted on the aged alloy in 0.5 M H_2SO_4 + 0.001 M TA (thioacetamid) solution proposed by Schultze et al.[18)] The degree of depletion in Cr and Mo in the alloy was evaluated by measuring the ratio of reactivation peak current (i_r) to activation peak current (i_a) when the potential was applied at a scan rate of 1 $mV\text{-}sec^{-1}$ from -500 to 200 mV_{SCE}, and then reversely to -500 mV_{SCE}.

Microstructure and phase compositions of the alloy were examined by a scanning electron microscopy (SEM) and an attached electron-dispersive X-ray spectroscopy (EDS). For microstructure observation, electrolytic etching was performed in 10 % KOH solution to distinguish phases. In addition, the precipitation of second phases in the alloy was detected by X-ray diffraction (XRD) using Cu K_α radiation.

3. Results and discusstion

3.1. Effects of aging on microstructure

Fig. 1 shows the optical micrographs of DSS aged respectively for 20 min, 1 h, and 10 h at 850 ℃. In the

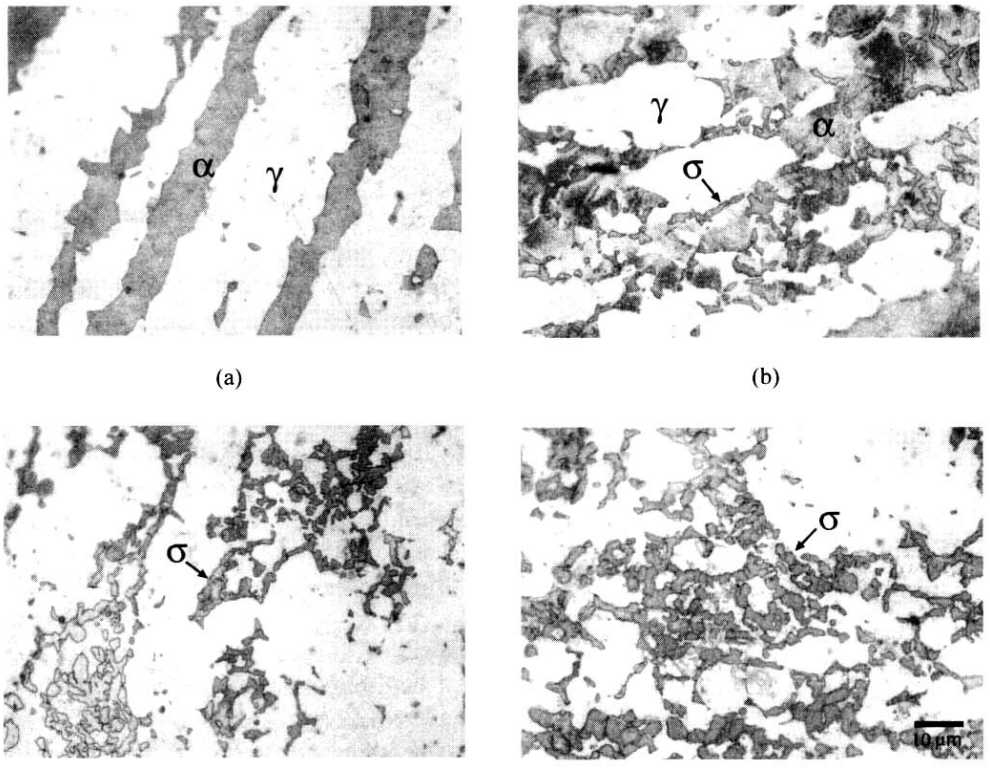

Fig. 1. Optical micrographs of the duplex stainless steels, which were (a) solution annealed and aged at 850 ℃ respectively for (b) 20 min, (c) 1h, and (d) 10h.

Fig. 1 (a) for the solution annealed alloy, dark phase indicates α and bright one does γ. In this case, no precipitates were found in grain or at grain boundaries. In the alloy aged for 20 min (Fig. 1 (b)), fine σ precipitates appeared at some α / α and α / γ boundaries, and in the alloy aged for 1 h (Fig. 1 (c)), the precipitates were found at most α / α and α / γ boundaries. Finally, in the alloy aged for 10 h (Fig. 1 (d), the size of σ precipitate at the boundaries was significantly increased. The volume fraction of the σ phase was evidently increased with an increase of aging time as shown in Table 2.

Fig. 2 shows the XRD pattern of the alloy subjected to aging for 1 h at 850 ℃ in which the diffraction peaks for α, γ, and σ phases were observed. The diffraction peaks for σ phase appeared distinctly around 42° of 2θ and weak between 45° to 50°. The chemical compositions of α, γ and σ phases in the alloy aged for 1 h were analyzed by SEM-EDS, and presented in Table 3. The contents of Cr and Mo in σ phase were much higher compared with those in neighboring α and γ phases. Due to high contents of Cr and Mo in it, the precipitation of σ phase depletes surrounding phases of Mo and Cr, leading to a reduction in corrosion resistance of DSS.[6)-9)] In order to correlate the precipitation of σ phase with the pitting susceptibility

Table 2. Volume fraction (%) of σ phase in the duplex stainless steel with aging at 850 ℃.

Aging time	S. A.	20 min	1 h	10 h
Volume fraction (%)	0	11	21	32

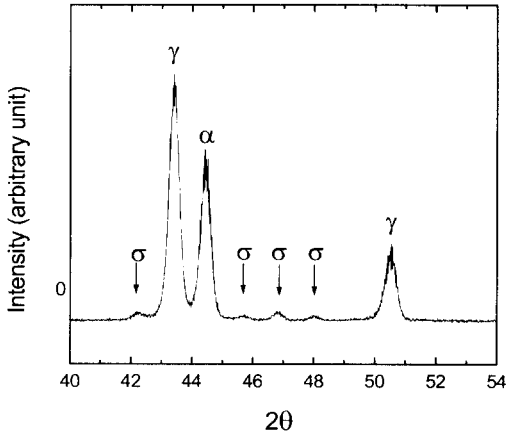

Fig. 2. XRD pattern, obtained by Cu K_α radiation, of the duplex stainless steel aged for 1 h at 850 ℃.

of the alloy, electrochemical potential and current noises were examined in the following sections.

3.2 Effect of aging on potential and current noises

Potential and current variation of the alloys aged at 850 ℃ for 20 min, 1h, and 10h were measured simultaneously with ZRA in 10 % $FeCl_3 \cdot 6H_2O$ solution at 60 ℃, and the results are presented in Fig. 3. The potential and current transients of the solution annealed sample, as shown in Fig. 3 (a), were stable overall compared with those of aged samples. These small potential transients, characterized by a quick potential drop followed by slow recovery, appear to be associated with the initiation and repassivation of metastable pit. However, those transients that may be associated with a nonmetallic inclusion were not common in all solution annealed samples. For the alloy aged for 20 min, a big potential or current transient was appeared simultaneously at about 1,800 sec. In contrast to the potential transient with the feature of quick drop followed by a slow recovery, the current transient is characterized by a quick anodic current rise followed by a slow decay.

Table 3. Chemical compositions (wt %) of α, γ and σ phases measured using SEM-EDS for the duplex stainless steel aged at 850 ℃ for 1 h.

	Fe	Cr	Ni	Mo
Ferrite (σ)	63.27	27.05	5.22	4.46
Austenite (γ)	65.48	24.29	7.67	2.56
Sigma (σ)	57.44	30.34	4.10	8.12

The abrupt decrease in the potential or the increase in the current is associated with a film breakdown process occurring in an event of metastable pit. The metastable pit may grow into a stable pit if the pit depth is by itself a sufficient diffusion barrier to maintain an environment that is sufficiently aggressive to prevent repassivation at the metal surface inside the pit. Sato[19] suggested that the corrosion potential of passive metal decreases as a metastable pit grows, and eventually become active state

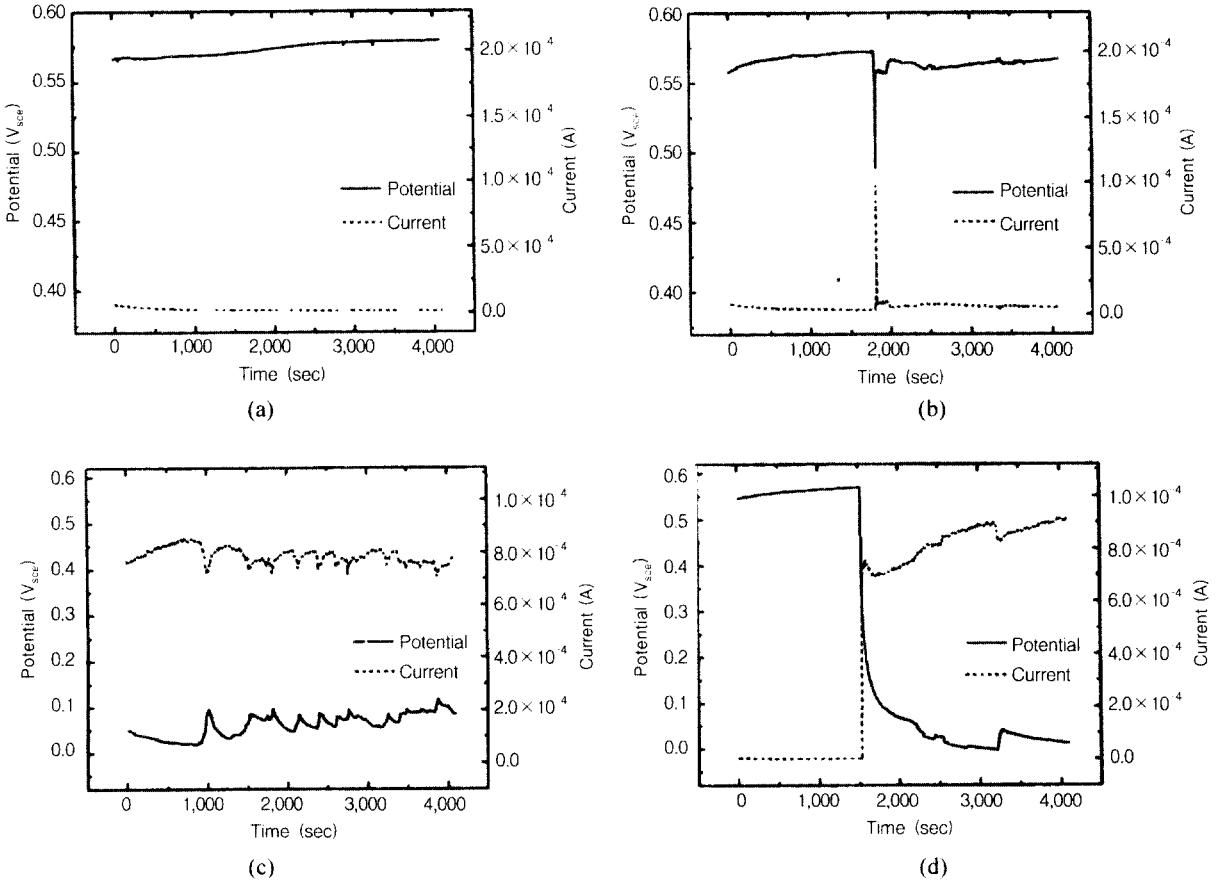

Fig. 3. Potential and current records vs. time of the duplex stainless steels (a) solution annealed and aged for (a) 20min, (b) 1h and (c) 10 h in 10 % $FeCl_3 \cdot 6H_2O$ solution at 60 ℃.

as the metastable pit grows into the a stable pit. For the metastable pit with insufficient pit radius and depth, the corrosion potential stops decreasing in active direction and then returns to the stable potential in passive state with the repassivation of pit.

Fig. 3 (c) and (d) show the potential and current transients measured simultaneously for the alloys respectively aged for 1 and 10 h. The potential of the alloys was more active and the corresponding current was more anodic than those of the alloy aged for 20 min. It suggests that for the alloy aged for longer than 1 h, pit grows stably in active state. Especially in Fig. 3 (d), the alloy aged for 10 h, the transition of pit growth mode from passive to active state was found near at 1500 sec of immersion time.

3.3. Power spectral density (PSD) analysis

To examine quantitatively the influences of aging on the electrochemical noise of the alloy, the electrochemical potential and current transients were transformed from time domain to frequency domain by MEM. Fig. 4 shows the PSD plot corresponding to the data shown in Fig. 3. De-trending was performed by a linear fitting method before converting to PSD because the mean potential and current of each alloy were quite different. On the whole, the potential and current PSD of the samples were getting higher with an aging. This is more prominent in the current PSD curves than in the potential PSD curves. The PSD curves of the samples aged for 1 h and 10 h were similar to each other, but the PSD of the alloy aged for 10 h in low frequency range was higher than that of the alloy aged for 1h. From the results, it was found that the passive film of DSS got significantly unstable with an increase in aging time. This seems to be related to the precipitation of σ phase during the aging at 850 ℃.

3.4 Corrosion admittance (A_c) spectrum

In addition, potential and current noises were analyzed in terms of corrosion admittance (A_c), which is defined as following equation.

$$A_c = \frac{\delta I}{\delta V} \quad (1)$$

In uniform corrosion, a positive, respectively negative, potential shift, δV at a certain moment belongs to a positive, respectively negative, current shift, δI. The ratio of their magnitudes thus leads to positive momentary corrosion admittance, A_c. On the other hand, in localized corrosion with breakdown of a passive film for instance, then a potential drop (negative δV) occurs simultaneously with an anodic current (positive δI), resulting a negative

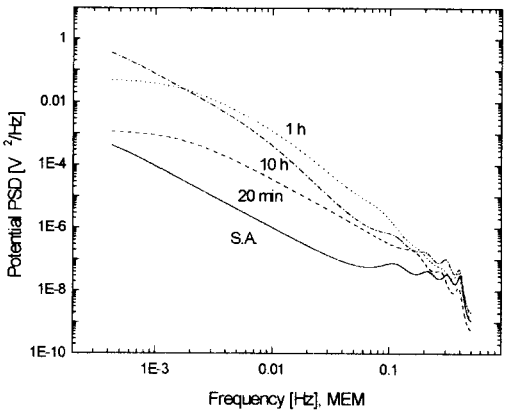

(a)

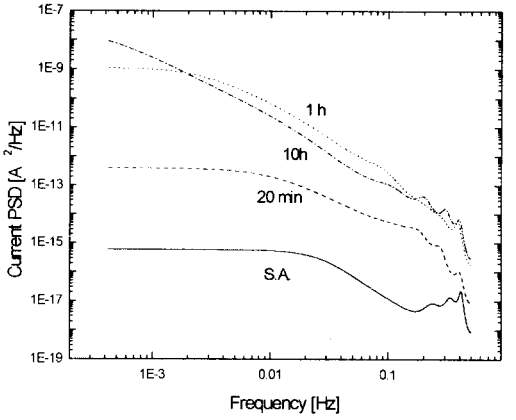

(b)

Fig. 4. (a) Potential and (b) current PSD of the aged duplex stainless steels determined from the potential and current noises in Fig. 3.

A_c. For repassivation in localized corrosion, however, the opposite phenomenon; positive δV and negative δI is found, with again a negative A_c. To distinguish the repassivation process from the film breakdown process, the A_c for the repassivation process was assigned to zero value even if a positive δV is detected in combination with a negative δI in the software.

Fig. 5 shows the A_c spectrum of the aged alloys determined form the potential and current transients in Fig. 3. The number of negative A_c event corresponding to a state of localized corrosion increased with aging, suggesting that the precipitation of σ phase considerably degrade the stability of passive film, thereby leading to pitting corrosion. In Fig. 5, the positive A_c was also frequently found in long-aged samples, which indicating that the breakdown of the passive film alternated with the active dissolution in the pit. Additionally, the deviation from zero A_c increased with aging, reflecting the increase of intensity

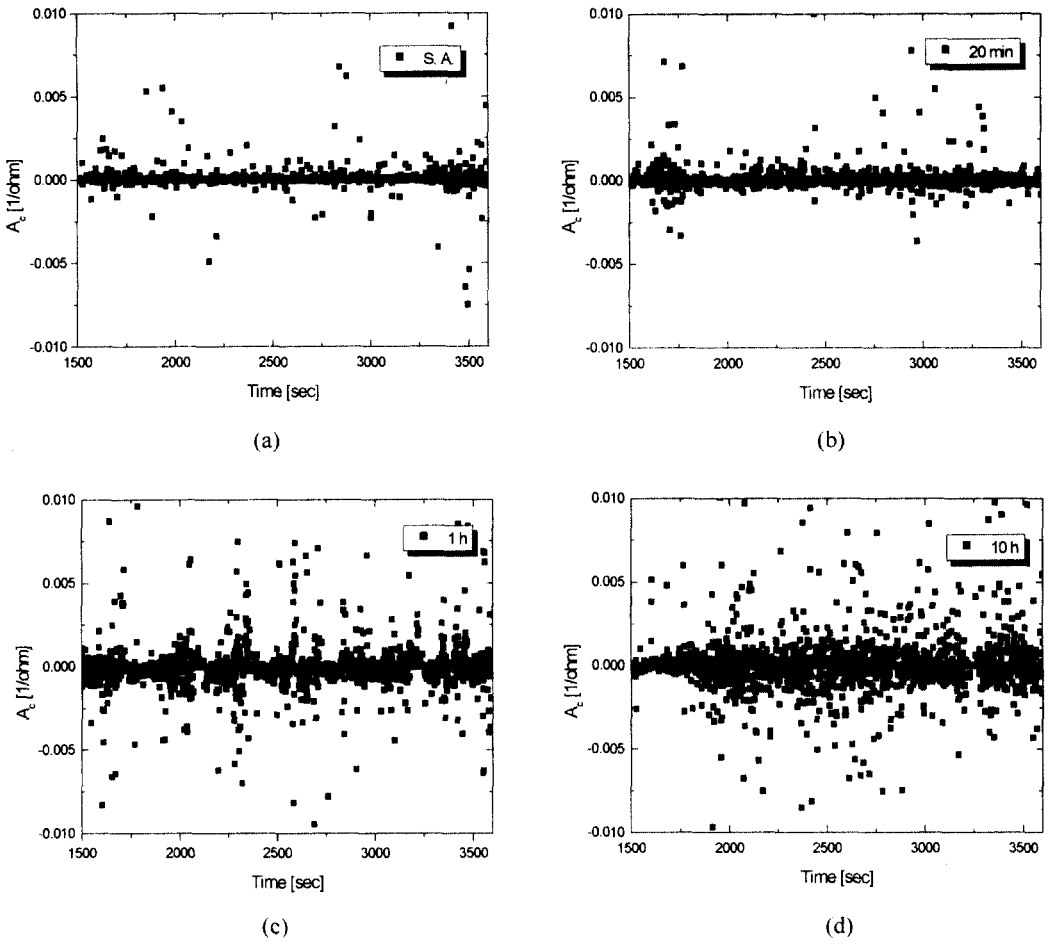

Fig. 5. Corrosion admittance spectrum of aged duplex stainless steels determined from potential and current records in Fig. 3; (a) Solution annealed, (b) Aged for 20 min, (c) Aged for 1h, and (d) Aged for 10 h.

for localized corrosion.

It is evident that the precipitation of σ phase played an important role in pit initiation by deteriorating the passive film around such phase, and consequently the overall resistance to pitting of DSS was degraded with aging. The transition from the metastable pitting state to the stable pitting state occurred at the aging time between 20min and 1 h. It appears that an effective size of δ phase is required for the propagation of metastable pitting.

3.5 Observation of pit morphologies

Fig. 6 shows the surface morphologies of the alloy aged for 1 h at 850 ℃ after noise measurement in 10 % $FeCl_3 \cdot 6H_2O$ solution. In Fig. 6 (a), pits with small size of 2~3 μm were found near α / σ phase boundaries, suggesting that the region around the σ phase was sensitive to the initiation of pit, where Cr and Mo were depleted. Theses pits are considered as metastable pits which were repassivated without the transition to stable pit. In contrast, Fig. 6 (b) shows a large cluster of stable pits. Pits were formed in sites where the σ phase precipitated densely. According to Williams et al.,[9] the resistance to pitting and crevice corrosion of 24.01Cr-7.11Ni-3.89N DSS in seawater was reduced on aging for longer than 7 min. They also reported that the initiation of localized corrosion took place around the σ phase as a result of the depletion of Cr and Mo, while the σ phase itself appeared unaffected. This was also confirmed in the present study by SEM observation of the pits shown in Fig. 6.

3.6 Double-loop electrochemical reactivation test (DL-EPR test)

The degree of sensitization of the alloy resulting from the depletion of Cr and Mo around σ precipitates with aging was examined by a double-loop electrochemical potentiokinetic reactivation (DL-EPR) tests conducted in 0.5M H_2SO_4 + 0.001 M TA (thioacetamid) solution at 60 ℃, and the results are presented in Fig. 7. The reactivation

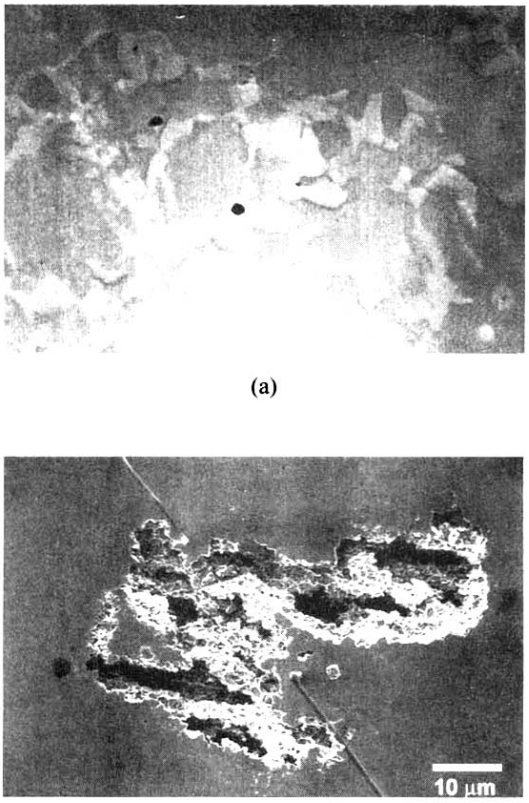

(a)

(b)

Fig. 6. SEM surface morphologies of the duplex stainless steels aged for 1h at 850 ℃ after electrochemical noise measurements in 10 % $FeCl_3 \cdot 6H_2O$ solution at 60 ℃; which showing (a) metastable pit and (b) stable pit.

current peak (i_r) was not appeared in the solution annealed sample, whereas a large reactivation current peak was obtained in the sample aged for 1 h as shown in Fig. 7 (b). Two current peaks observed at -0.28 V_{SCE} and -0.32 V_{SCE} for the solution annealed sample during the reactivation potential scanning resulted respectively from hydrogen reduction reaction and metal dissolution reaction.

The degree of sensitization of the alloy with aging was determined from the ratio of reactivation peak current (i_r) to activation peak current (i_a) in the double loop EPR tests as shown in Table 4. The i_r / i_a ratio is closely associated with the depletion of Cr and Mo around the σ phase. The reactivation peak was not observed in the alloys which were aged for less than 1 h. It is noticeable that the ir/ia ratio of the alloy aged for 1 h ($i_r / i_a = 0.030$) was measured to be higher than that of the alloy aged for 10 h ($i_r / i_a = 0.015$). This suggests that the Cr and Mo in the α / σ or γ / σ phase boundaries which were once depleted resulting from the precipitation of the σ phase were partly replenished by the diffusion of Cr and Mo from the

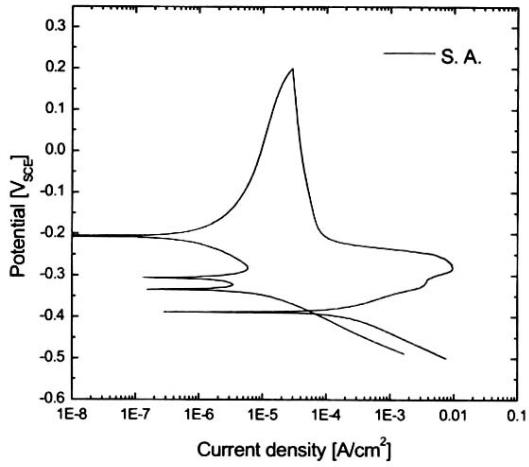

(a)

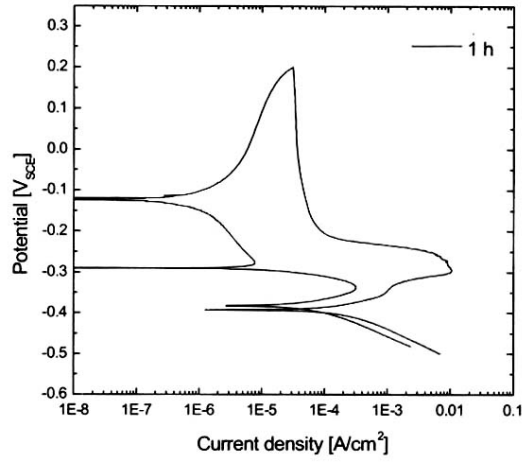

(b)

Fig. 7. Double-loop electrochemical potentiokinetic reactivation (DL-EPR) curves for the duplex stainless steel in 0.5 M H_2SO_4 + 0.001 M TA (thioacetamid) solution at 60 ℃; (a) solution annealed and (b) aged for 1 h.

Table 4. The degree of Cr-depletion of the duplex stainless steel with aging at 850 ℃ in terms of the reactivation activation current peak ratio (i_r / i_a) determined from the DL-EPR tests.

Aging time	S. A.	20 min	1 h	10 h
i_r / i_a	0	0	0.030	0.015

surrounding matrix with an increase of aging time. However, the results are contrary to the fact that the PSD in the low frequency region and the A_c value of the alloy aged for 10 h were higher than that of the alloy aged for 1 h, which reflecting that the sensitivity to the localized corrosion increased with an increase of the aging time.

The answer to the question can be given in an aspect

of the precipitation density of the σ phase. From Fig. 1 and the table 1, it was found that the volume fraction of the σ phase increased with an increase of aging time. This suggests that the number of sites for the initiation of pitting increased with an increase of the area of the α / σ or γ / σ phase boundaries, which were preferential sites for pitting. Thus, it is considered that the precipitation density of σ phase as well as the degree of sensitization is also important for pit initiation in DSS.

Consequently, the initiation of pitting seems to be closely associated with the precipitation density of the σ phase with an effective size which is enough to induce the sufficient depletion of Cr and Mo around it.

4. Conclusions

1) With an aging at 850 ℃, the σ phase, enriched in Cr and Mo, precipitated along α / α and α / γ boundaries in the Fe-25Cr-7Ni-3Mo-0.25N alloy, and the volume fraction of the σ phase increased with an increase in aging time.

2) The potential and current transients, which were associated with the initiation and the following repassivation of the metastable pitting, were observed on the aged alloy in a highly aggressive chloride solution. For the alloy aged for longer than 1 h, it was found that the pit grew stably in active state. The susceptibility to the pitting seems to be closely related to the precipitation of the σ phase with aging.

3) The PSD curves corresponding to the potential and current noises confirmed that the passive film of the alloy got unstable with aging due to the depletion of Cr and Mo around the σ phase.

4) In the corrosion admittance (A_c) spectrum, the number of negative A_c corresponding the state of localized corrosion increased with aging, suggesting that the σ phase considerably degrade the passive film, thereby leading to the initiation of the pitting. In addition, the deviation from zero A_c increased with aging, reflecting the increase of the severity of the localized corrosion.

5) The α / σ or γ / σ phase boundaries were revealed to be susceptible to the initiation of the metastable pit due to the depletion of Cr and Mo around the σ phase. However, the Cr and Mo at α / σ or γ / σ phase boundaries which were once depleted resulting from the precipitation of the σ phase were partly replenished by the diffusion of Cr and Mo from the surrounding matrix with an increase of aging time.

6) The initiation of pitting seems to be associated with the precipitation density of the σ phase with an effective size which can induce the sufficient depletion of Cr and Mo around it.

References

1. R. F. Steigerwald, *Corrosion* **33**, 338 (1977).
2. C. J. Park and H. S. Kwon, "Effects of aging at 475 ℃ on the corrosion of W-containing duplex stainless steels", Proceedings, Vol. 2, The 11th Asian-Pacific Corrosion Conference, Ho chi minh, Vietnam 870 (1999).
3. J. O. Nilsson, *Mater. Sci. Tech.* **8**, 685 (1992).
4. C. S. Barret and T. B. Massalski, Structures and Metals, 3rd ed., Oxford, U. K. Pergamon Press 266 (1980).
5. R. G. Barrows, J. B. Newkirk, *Metall. Trans. 3* **2**, 889 (1972).
6. J. O. Nilsson and A. Wilson, *Mater. Sci. Tech.* **9**, 545 (1993).
7. K. Ravindranath and S. N. Malhotra, *Corros. Sci.* **37**, 121 (1995).
8. K. Ravindranath and S. N. Malhotra, *Corrosion*, **50**, 318 (1994).
9. M. E. Williams, V. J. Gadgil, J. M. Krougman and F. P. Ijsseling, *Corros. Sci.* **36**, 87 (1994).
10. Z. Szklarska-Smialowska and E. Lunarska, *Werst. Korros.* **32**, 478 (1981).
11. J. S. Kim and H. S. Kwon, *Corrosion*, **55**, 512 (1999).
12. G. T. Burnstein, P. C. Pistorius and S. P. Mattin, *Corros. Sci.* **35**, 57 (1993).
13. D. L. Reichert, "Electrochemical noise measurement for determining corrosion rates", Electrochemical noise measurement for corrosion applications, ASTM STP 1277, Jeffery R. Kearns, John R. Scully, Pierre R. Roberge, David L. Reichert, and John L. Dawson, Eds., American Society for Testing and Materials, pp 79-89 (1996).
14. P. C. Pistorius, "The effect of some fundamental aspects of the pitting corrosion of the pitting corrosion of stainless steel on electrochemical noise measurements", Electrochemical noise measurement for corrosion applications, ASTM STP 1277, Jeffery R. Kearns, John R. Scully, Pierre R. Roberge, David L. Reichert, and John L. Dawson, Eds., American Society for Testing and Materials, pp.343-358 (1996).
15. H. Böhni, T. Suter, and A. Schreyer, *Electrochim. Acta* **40**, 1361 (1995).
16. S. Haykin, Adaptive Filter Theory, second ed., Prentice Hall, Engelwood Cliffs, NJ, p.798 (1991).
17. J. Hubrecht, R. -W Bosch, J. Chen, W. Bogaerts, and J. H. Zheng, Proceedings, Vol. 1, The 11th Asian-Pacific Corrosion Conference, Ho chi minh, Vietnam pp.126-150 (1999) .
18. S. Shultze, J. Golner, K. Eick, P. Veit, and I. Garz, 5th World Conf. Duplex Stainless Steels 97, Maastricht, the Netherlands, pp.639-648 (1997).
19. N. Sato, *Corros. Sci.* **37**, 1947 (1995).